Energy & Environmental Science

View Online Dynamic Article Links

Cite this: *Energy Environ. Sci.*, 2011, **4**, 2090

www.rsc.org/ees

PAPER

Reevaluation of $PbTe_{1-x}I_x$ as high performance n-type thermoelectric material

Aaron D. LaLonde,† Yanzhong Pei† and G. Jeffrey Snyder*

Received 18th March 2011, Accepted 26th April 2011
DOI: 10.1039/c1ee01314a

Thermoelectric transport properties of n-type $PbTe_{1-x}I_x$ with carrier concentrations ranging from 5.8 $\times 10^{18}$–1.4 $\times 10^{20}$ cm^{-3} are reinvestigated from room temperature to 800 K. The electronic transport properties, resistivity and Seebeck coefficient in this study are effectively consistent with prior reports, however the thermal conductivity has been found to be historically overestimated. The reassessment of the thermal transport properties, in combination with careful control of the carrier density by iodine doping, reveals a significantly larger figure of merit, $zT \sim 1.4$, than often previously reported for n-type PbTe. The results and analysis of the data from this study lead to a redetermination of zT for this historical thermoelectric material and provide a renewed interest in n-type PbTe based materials.

1 Introduction

Lead telluride and its alloys have played a critical role in the development of thermoelectric power generation applications for more than 50 years,[1] typified by the successful demonstration of NASA's Apollo program.[2] The recent research efforts, largely focused on nano-structures for effective phonon scattering, have resulted in several examples of the thermoelectric figure of merit reaching much higher than unity.[3–7] The metric by which the performance of a thermoelectric material is measured is the thermoelectric figure of merit, $zT = (S^2T)/(\rho(\kappa_E + \kappa_L))$, where S, ρ, κ_E, and κ_L are respectively the Seebeck coefficient, electrical resistivity, and electronic and lattice contribution to thermal conductivity. Lead chalcogenides have low thermal conductivity and excellent electronic transport properties required for high performance thermoelectric materials.[1,8–10] However, historically, there were very few well documented thermal conductivity measurements on n-type PbTe, in contrast to the sophisticated measurements of the electronic properties and band structure led by Soviet Union scientists.[1,8,11]

Much of the early thermal characterization on thermoelectric materials, including PbTe, was done using an absolute steady state method[12] best suited for measurements below room temperature, becoming susceptible to measurement error in the medium to high temperature range. In the 1960s when PbTe materials were extensively investigated as a thermoelectric material[8] it was well known that accurate characterization of thermal conductivity at high temperature was difficult.[13] Early studies, such as the seminal work on PbTe by Fritts,[14] used room temperature lattice thermal conductivity data for zT calculation extrapolated to elevated temperatures. Without a doubt, this method resulted in an overestimated lattice thermal conductivity and therefore an underestimated zT, as it is known that the lattice thermal conductivity should decrease roughly with $1/T$ due to the

Materials Science, California Institute of Technology, Pasadena, California, 91125. E-mail: jsnyder@caltech.edu
† Authors have contributed equally to this work.

Broader context

For over 50 years PbTe based thermoelectrics have been used to produce electricity on NASA missions. The cover image of this issue shows a radioisotope thermoelectric generator containing PbTe with essentially the same composition of that reinvestigated here. As in the preceding article on p-type PbTe, the thermoelectric performance of n-type PbTe was also underestimated historically due to the difficulties on accurate estimation of the thermal conductivity. This underestimate resulted in the peak thermoelectric figure of merit, zT, of ~0.8 obtained from the early research in the 1960s being commonly referenced to this day as the optimized value for n-type PbTe. Reinvestigation of this simple material reveals that with precise doping control and use of modern thermal conductivity characterization, the material system actually shows zT as large as ~1.4 at high temperatures. Both the preceding and current report in this issue collectively show that such high zT values are intrinsic to PbTe if properly doped. With the reliability of PbTe proven in space, these simple n- and p-type materials should be the basis for comparison during the evaluation and development of thermoelectric waste heat recovery technology on Earth.

Umklapp scattering of phonons at high temperatures.[8] Analogously, it has been recently pointed out that this assumption led to severely underestimated peak zT values (~0.7) in the p-type Na-doped PbTe where the actual optimal value is ~1.4.[11] The same assumption for thermal conductivity at elevated temperature has led to an equally underestimated peak zT (~0.8) in n-type PbI_2 doped material as well (referred to as $PbTe_{1-x}I_x$ in this report), and it is reported here that the actual zT value is ~1.4 between 700–800 K with the proper doping level.

Historically the n-type PbTe that has been most used by NASA for powering space crafts was referred to as "2N" and "3N".[2] This material was developed by the 3M corporation (Fritts) and the exact details on the processing of these alloys are not well publicized. However, it was known that the n-type material was typically prepared by adding PbI_2 to the base PbTe compound, with the 2N composition containing 0.076 wt% PbI_2 (~x = 0.0010), and 0.14 wt% (~x = 0.0020) for the 3N composition.[15] The zT values of Fritts' material (~0.8) matched that for 2N and 3N and was therefore assumed to be accurate. The data reported by Fritts has been widely reported to date and is believed to be accurate for PbI_2 doped PbTe.[2,5,16–23] This n-type PbTe is contained in the only commercially available (Global Thermoelectric) thermoelectric generators operating above 525 K, and is therefore most developed for use in waste heat recovery applications.

Although the commonly referenced peak zT for n-type PbTe is ~0.8, there are various reports in the literature showing zT ~ 1.[8,24–26] Kudman has reported zT values for 2N and 3N materials of ~1 using a high temperature thermal diffusivity measurement system.[27] Gelbstein has reinvestigated iodine doping of PbTe using previously reported thermal conductivity data to obtain zT ~ 1.1.[25,26] The total thermal conductivity of nanostructured $Pb_{1-x}Sn_xTe$–PbS doped with 0.055 mol% PbI_2 has recently been investigated using flash diffusivity and finds κ ~ 1 W m^{-1} K^{-1} near 700 K, compared to Fritts' reported values of ~1.9 W m^{-1} K^{-1} for iodine doped PbTe.[28] Similar materials in the PbTe–CdTe system have recently been studied using the flash diffusivity technique as well, reporting total thermal conductivity values κ ~ 1 W m^{-1} K^{-1} for the samples with the smallest amount of Cd alloying (1%).[29] The zT values reported in the $Pb_{1-x}Sn_xTe$–PbS system ranged from 1–1.5 at 650 K and were just less than 1.2 at 720 K in the PbTe–CdTe system. The work done in our study uses the same technique for thermal conductivity measurement that has commonly been used in the field of thermoelectrics since the 1990s. To date, there does not exist research that combines the optimized carrier concentration from the initial historic research for basic n-type PbTe combined with the flash diffusivity technique for accurate thermal characterization.

In this report we confirm the electronic transport properties of S, ρ and n of similar compositions to those reported in the past for n-type PbTe doped with PbI_2, as well as additional samples across the doping range as an attempt to more carefully control the carrier density. The high temperature thermal conductivity is measured to 800 K enabling a more accurate determination of a peak zT ~ 1.4 from 700–800 K, a significant difference from the assumption of a maximum zT of ~0.8. Such a careful reinvestigation additionally provides a complementary explanation for recently reported high zT values in n-type PbTe thermoelectric materials.[3–6]

2 Experimental

Polycrystalline samples of $PbTe_{1-x}I_x$ (x = 0.0004, 0.0007, 0.0012, 0.0020, 0.0028, 0.0040, 0.0055 and 0.0100) were prepared by appropriately mixing end compounds with the stoichiometry PbTe and $PbTe_{0.99}I_{0.01}$. The end compounds were prepared by melting the stoichiometric ratio of elemental Pb, Te and PbI_2 in vacuum sealed quartz ampoules at 1273 K for ~6 h followed by water quenching. The PbTe and $PbTe_{0.99}I_{0.01}$ were used to prepare the $PbTe_{1-x}I_x$ samples which were sealed in quartz ampoules, melted at 1273 K for 6 h, water quenched and annealed at 973 K for 48 h. The annealed ingots were hand ground to powder and were consolidated at 823 K for 60 min under a pressure of 44 MPa by induction hot pressing.[30] The resulting samples are greater than 98% theoretical density. The Seebeck coefficient was calculated from the slope of the thermopower *vs.* temperature gradient measurements from Chromel-Nb thermocouples, resistivity and Hall coefficients were measured using the Van der Pauw technique under a reversible magnetic field of 2 T, and the thermal diffusivity measurement was made by the laser flash method (Netzsch LFA 457). All measurements were performed under vacuum. Heat capacity (C_p) was estimated by C_p (k_B per atom) = 3.07 + 4.7 × 10^{-4} × (T/K − 300), obtained by fitting experimental data reported by Blachnik[31] within an uncertainty of 2% for all the lead chalcogenides at T > 300 K giving C_p ~ 10% higher than the Dulong-Petit limit value at T > 700 K, as previously reported.[7,11] It should be emphasized that this simple equation agrees well with the theoretical prediction taking the lattice vibration, the linear coefficient of thermal expansion and charge carrier contributions into account.[11] The combined uncertainty for all measurements involved in zT determination is ~20%.

It is important to ensure that the nomenclature used to describe the composition of the materials in different reports is understood so that a meaningful comparison can be made. Based on a comparison of our transport data to that reported by Fritts, we deduce that Fritts interprets mol% of PbI_2 to mean the number of moles of PbI_2 (3 atoms/molecule) out of the number of moles of PbTe (2 atoms/molecule). This interpretation gives the number of moles of PbI_2 to be ~x/2 in the formula $PbTe_{1-x}I_x$ (for example, Fritts' 0.03% PbI_2 corresponds to x = 0.0006). Based on the table that Gelbstein gives[56] and the transport properties reported, it is consistent that his interpretation of mol % PbI_2 is the number of moles of PbI_2 molecule relative to the number of moles of each Pb and Te individually. Gelbstein's interpretation gives the number of moles of PbI_2 to be ~x/4 in $PbTe_{1-x}I_x$ (for example, Gelbstein's 0.03% PbI_2 corresponds to x = 0.0012). In this report the form $PbTe_{1-x}I_x$ is used.

It should be noted that nearly all previous reports on n-type PbTe doped with iodine contain an excess of Pb (>50 atomic %) in composition. Excess lead is added in order increase the mechanical strength over that of the stoichiometric material and to help ensure reproducible electrical properties.[14] Having an excess of Pb should lead to Te vacancies and n-type carriers on the order of 3 × 10^{17}–1.7 × 10^{18} cm^{-3}, while further including additional doping elements will allow carrier concentrations on the order of 10^{20} cm^{-3}.[14] As the excess Pb is not necessary to obtain the desired doping levels for PbTe, the material for this study has been made in the stoichiometric composition. By

investigating the stoichiometric composition the results are not expected to be attributed to any effects of having excess Pb present, such as the presence of nanometre sized precipitates[32] or temperature dependent carrier concentration.[7]

3 Results and discussion

The measured negative Hall coefficients indicate the n-type conduction for all samples made in this study. The calculated Hall carrier concentrations ($n_H = 1/eR_H$) are shown and compared in Fig. 1 to the calculated values assuming each substitutional I atom releases one extra free electron into the conduction band due to the valence rule.[33] It is seen that iodine acts effectively as a 1 : 1 dopant when substituted for Te and is capable of precisely controlling the carrier concentration in PbTe. For this study, carrier concentrations ranging from 5.8×10^{18}–1.4×10^{20} cm^{-3} were obtained. The undoped PbTe made for this study had n-type conduction with a carrier concentration of 1.11×10^{18} cm^{-3}.

The measured values of the Seebeck coefficient and resistivity up to 800 K for the samples in this study are shown in Fig. 2 and 3. With increasing temperature, the linearly increasing absolute Seebeck coefficient and the monotonically increasing resistivity suggest degenerate semiconducting behavior for the majority of the samples here. These trends, combined with the observation of a slightly increased Hall coefficient as temperature increases (which can be expected from a slight loss of degeneracy as temperature increases), allow the assumption of single band conduction behavior for most of the samples within the carrier concentration and temperature ranges studied.

An effective method that has been widely adopted for PbTe[8,34–36] and PbSe[37] to obtain meaningful insight regarding the carrier scattering mechanism and the band structure is to analyze the carrier density dependent Seebeck coefficient (the so-called Pisarenko relationship). The majority of the reported Seebeck coefficient data show a similar carrier density dependence at a given temperature, for both n-type[36] and p-type[34,35] PbTe. The data from the current study for the room temperature Seebeck coefficient *vs.* carrier density is shown in Fig. 4 along with

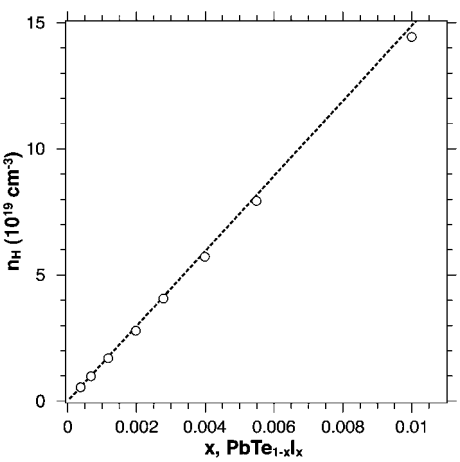

Fig. 1 Room temperature Hall carrier concentration for $PbTe_{1-x}I_x$ for the 8 compositions reported in this study. The dashed line is the expected carrier concentration for 1 e$^-$ per I atom.

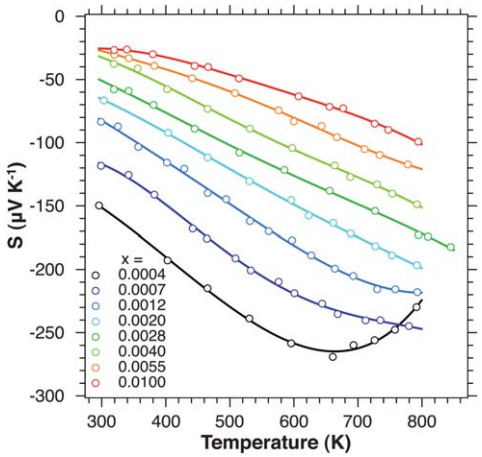

Fig. 2 Temperature dependent Seebeck coefficient for $PbTe_{1-x}I_x$.

reported values for comparison. At 300 K the values from this study are shown to be in agreement with historically reported values for the same material, indicating no significant change in the electronic transport properties by iodine doping of PbTe. Moreover, the Seebeck coefficient *vs.* carrier density relationship can be predicted well from a single Kane band model (solid curve) which takes the band nonparabolicity effect into account as carrier concentration and temperature increase.[8,38,39] It should be noted that this model assumes carrier scattering dominated by acoustic phonons in the temperature range studied.[8,38] The model also takes into account the temperature dependent density of states mass m^* at the conduction band edge of $d\ln m^*/d\ln T = 0.5$[7,8,40] and band separation of $E/eV(T) = 0.18 + 4T/10000$.[41–43] Additionally, the band anisotropy factor is assumed to be ~3.6 and temperature independent.[7,40] The details of the single Kane band model can be found elsewhere.[8] The Kane band model describes the high temperature S *vs.* n_H data very well, as shown in Fig. 4.

In addition, the theory of acoustic scattering[44,45] enables an accurate prediction of the carrier mobility based on a single Kane band model[8] when the deformation potential coefficient (E_{def}), which defines the strength of the scattering of carriers by acoustic

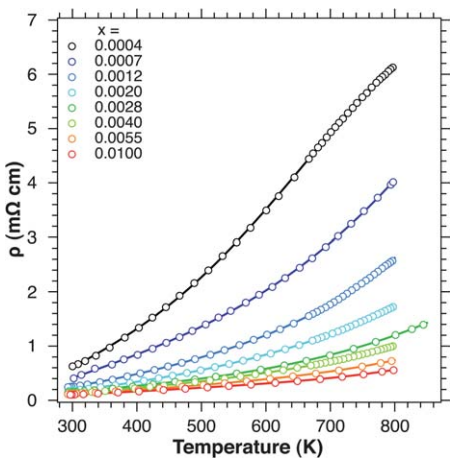

Fig. 3 Electrical resistivity as a function of temperature for $PbTe_{1-x}I_x$.

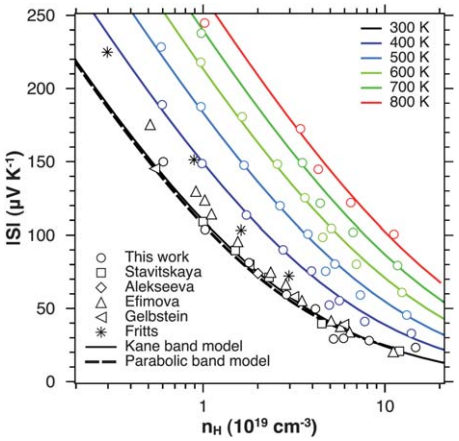

Fig. 4 Carrier concentration dependent Seebeck coefficient for $PbTe_{1-x}I_x$ at several temperatures. Room temperature values from this study are compared to those reported in the literature.[14,25,52–54] Carrier concentration was not reported by Fritts or Gelbstein and was therefore assumed to be the predicted value based on the absolute iodine concentration from the compositions reported.

phonons, is known. Using the knowledge that the conduction band minima of PbTe occurs at the L -point of the Brillouin zone with a valley degeneracy of 4,[8,46–48] the electronic transport data fit to the Kane band model determines the value of E_{def} to be in the range of 22 ± 2 eV in the extrinsic conduction region. The room temperature mobility *vs.* carrier density is shown in Fig. 5 and compared to literature results.

For comparison, Fig. 4 and 5 also include the model predictions (dashed curves) of carrier density dependent Seebeck coefficient and mobility at room temperature assuming a single parabolic band (SPB) model, which does not take the band nonparabolicity into account. The details about the SPB model under acoustic scattering can be found elsewhere.[8,49] Even though the SPB model enables an equally accurate prediction of the Seebeck coefficient as the SKB model[7] (Fig. 4), using the same m^* of $0.25m_e$ and the same E_{def} of 22 eV, the carrier density dependent mobility (Fig. 5) can be better explained by the Kane band model, especially at higher doping levels where the band nonparabolicity effect is stronger. This is consistent with the previously reported conclusion that the L bands for lead chalcogenides are nonparabolic and can be approximated by the shape of a Kane band.[7,36,38,39,50,51]

It is clear that both the carrier concentration and temperature dependent electronic transport properties in the present work are consistent with the data reported by Gelbstein and Fritts. Shown in Fig. 6 are selected data from the literature that are commonly cited for n-type PbTe. In the temperature range where maximum zT values are expected (700–750 K) the sample from the current study has a resistivity value ~20% lower than the compared literature reports and a Seebeck coefficient ~10% lower, most likely due to slightly different dopant concentrations. The combined result of these differences minimally affect the power factor (S^2/ρ) and result in a difference of ~5% at high temperatures. A significant increase in the value of zT should, therefore, not be attributed to an increase in the power factor for these materials and is entirely due to the difference in thermal conductivity.

The measured total thermal conductivity for all $PbTe_{1-x}I_x$ samples is shown in Fig. 7. It has been shown that iodine acts as an effective electron donor (Fig. 1) thereby decreasing the resistivity due to the increased carrier concentration (Fig. 3). This decrease in resistivity results in an increase in the electronic component of the thermal conductivity (κ_E) and therefore an increase in the total thermal conductivity (Fig. 7), as this term is calculated by the Wiedemann-Franz law ($\kappa_E = LT/\rho$) where L is the Lorenz number.

The highest average zT is achieved in the composition of $x = 0.0012$ of this study and will therefore be the focus of the following discussion on the thermal transport properties. Additionally, this composition and carrier concentration is very often found reported in the literature data for thermal conductivity as shown in Fig. 8,[14,25,53,54] and provides an excellent comparison for discussion.

Among similar iodine doped PbTe one can clearly see the total thermal conductivity measured by the laser flash thermal diffusivity method in the present study shows an ~30–35% lower value than that of the steady state method over the whole

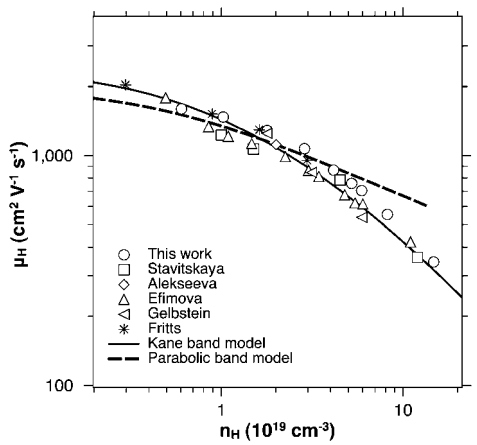

Fig. 5 Room temperature carrier concentration dependent Hall mobility for $PbTe_{1-x}I_x$. The values from this study are compared to those reported in the literature.[14,25,52–54]

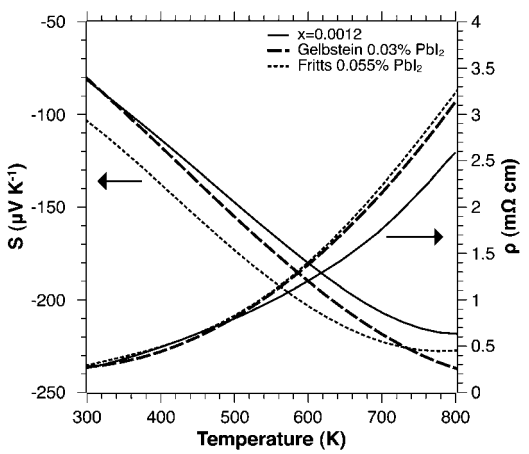

Fig. 6 Comparison of Seebeck and resistivity values for samples of similar compositions from the present work and literature.[14,25]

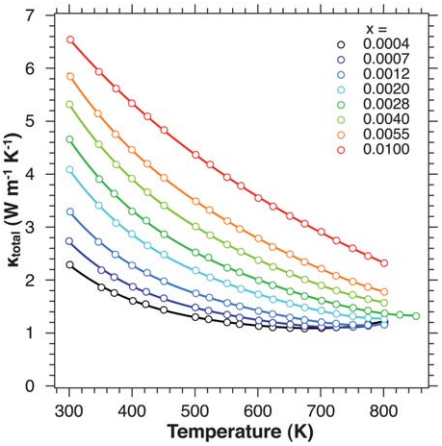

Fig. 7 Total thermal conductivity as a function of temperature for $PbTe_{1-x}I_x$.

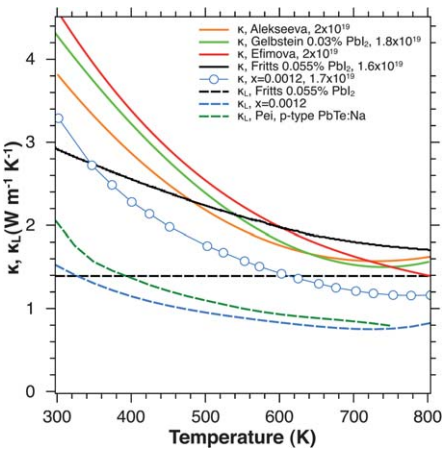

Fig. 8 Comparison of total thermal conductivity from literature and the present study.[14,25,53,54] Also shown are the lattice component of thermal conductivity assumed by Fritts, the values from this study for the sample $x = 0.0012$, and the values from the recently reported PbTe:Na p-type material.[11] Data from similar carrier concentration values are shown.

temperature range studied.[14,25,53,54] The data estimated by Fritts shows a different trend because a temperature independent lattice thermal conductivity value is assumed. Such a large discrepancy between total thermal conductivity values will lead to a significant difference in the determination of the lattice component of the thermal conductivity in contrast to the electronic transport data which show excellent agreement with previous reports.

An estimation of L and its temperature dependence can be made using the same Kane band model used to describe the electronic transport properties to determine κ_E for n-type PbTe materials.[8,39,55] The estimation of the lattice component of the thermal conductivity (κ_L) for the sample $x = 0.0012$ is shown in Fig. 8. The lattice thermal conductivity is determined by subtracting the electronic component from the total thermal conductivity, $\kappa_L = \kappa - \kappa_E$. The estimated lattice thermal conductivity value at room temperature is ~1.5 W m^{-1} K^{-1} and ~0.75 W m^{-1} K^{-1} at 750 K. These values are in close agreement with recently reported κ_L values for p-type PbTe materials measured using the same laser flash method,[11] also shown in Fig. 8. In each of these n- and p-type PbTe cases the materials are heavily doped.

In the study reported by Fritts[14] the temperature independent lattice thermal conductivity of 1.4 W m^{-1} K^{-1} (0.055% PbI_2, $\sim x = 0.0012$) and non-degenerate L (1.5×10^{-8} W Ω K^{-2}) was used and resulted in an overestimation of the total thermal conductivity, shown in Fig. 8. This overestimation in κ, needless to say, leads to significantly underestimated values of zT, particularly at high temperatures.

In the study reported by Gelbstein, showing a peak $zT \sim 1.1$, κ was not measured.[25] The electronic component of the thermal conductivity was calculated from measured resistivity data, the Wiedemann-Franz law ($L \sim 2.44 \times 10^{-8}$ W Ω K^{-2}), and subsequently combined with the calculated lattice component. The lattice component in Gelbstein's study was calculated using an expression derived from published data obtained from the steady state method below 400 K.[8] This method of thermal conductivity measurement is known to be sensitive at high temperature,[11,13] evident in Fig. 8. This point of vulnerability in the material characterization is also present in a considerable amount of older research reports.[52–54]

The zT values for all samples in this study are shown in Fig. 9. It is seen that as the doping concentration increases the peak zT increases, as well as the temperature of the peak. A peak zT of 1.4 is observed at about 750 K for samples with $x = 0.0012$–0.0020. The sample $x = 0.0028$ was remeasured to 850 K and shows zT slightly greater than 1.4 at $T > 800$ K.

Shown in Fig. 10, the zT values for the sample $x = 0.0012$ are compared to zT values reported in literature for samples of similar carrier concentration and composition. Also shown in Fig. 10 are the zT values from the literature that have been recalculated using the originally reported S and ρ values in combination with the L values for κ_E and lattice thermal conductivity from the current study for the sample $x = 0.0012$. Both the original (dashed lines) and the recalculated (solid lines) results are shown. It can be seen that the recalculation results in peak zT values differing by ~25–35% (same level of thermal conductivity variation). It can also be seen that the 2N data reported by Kudman (Fig. 10) shows excellent agreement with our $x = 0.0004$ sample (Fig. 9) in the entire temperature range,

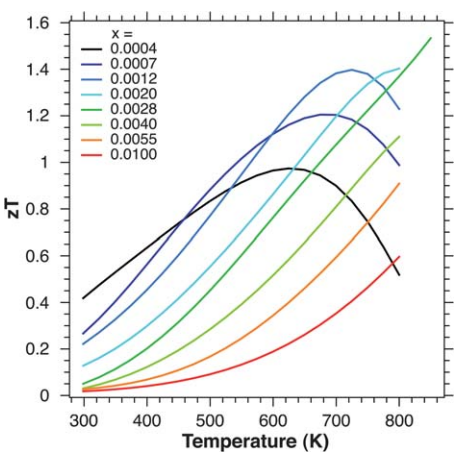

Fig. 9 Figure of merit, zT, as a function of temperature for $PbTe_{1-x}I_x$.

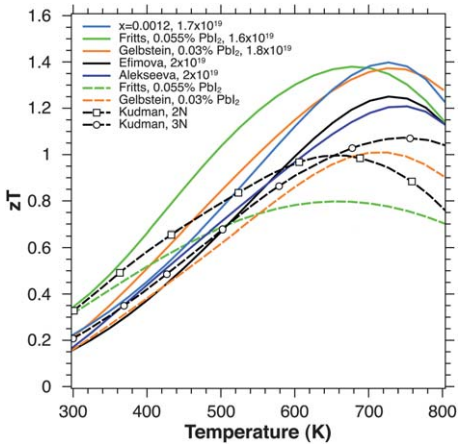

Fig. 10 Comparison of reported zT values from literature of similar carrier concentration values. The dashed lines are the original reported values.[8,14,25,52–54] The solid lines are estimated values using the electronic transport properties reported in the literature combined with the thermal conductivity values for the sample $x = 0.0012$ from the current study.

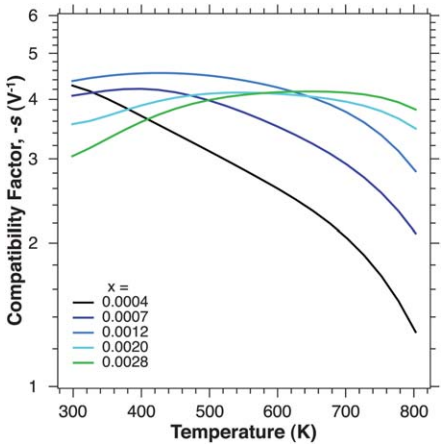

Fig. 11 Compatibility factor, s, for $PbTe_{1-x}I_x$.

suggesting the historical 2N material is probably under-doped. By further increasing the carrier density, both the peak and average zT can be realized as shown in Fig. 9. The samples being compared are close in carrier concentration and composition and show recalculated peak $zT \sim 1.2$–1.4 at high temperatures, a significant difference from the value of $zT \sim 0.8$ that is generally believed.

An additional 10 gram sample of the $x = 0.0012$ composition was prepared and consolidated into a cylinder ~10 mm tall. One sample was cut across the top of the cylinder and another sample along the length of the cylinder. The resistivity of these two samples was measured to 850 K and show a difference of <5%, which is within the uncertainty of the resistivity measurement, eliminating possible contributions from anisotropy effects induced by the uniaxial hot pressing technique. It is also noted that the sample $x = 0.0012$ has been made on 3 different occasions from separate alloy ingots and show minimal (<5%) variation in properties. One of the additional batches of material was made as the composition reported by Gelbstein's 0.03% PbI_2 ($x \sim 0.0012$)[56] which contains excess Pb and the measured properties were not affected by the non-stoichiometry of the material. The mechanical strength of the materials reported in this study have not been tested. X-ray diffraction was done in an effort to confirm the phase purity of the samples and no evidence was found that would suggest the presence of any secondary phases. Additionally, it has been previously reported that there is no significant difference between single crystal and polycrystalline samples of n-type PbTe.[53]

The precisely and uniformly changing properties make iodine doped PbTe ideal for functionally grading thermoelectric material.[25,26,56] Fig. 11 shows the power generation compatibility factor $(s = (\sqrt{(1+zT)}-1)/(ST))$ of the highest performing (zT) $PbTe_{1-x}I_x$ samples which is needed for optimal selection of materials for segmentation and functionally grading.[57] To achieve maximum efficiency in a segmented element, materials with similar compatibility factors (differing by less than a factor of 2) are required. It can be seen that the n-type $PbTe_{1-x}I_x$ materials from this study are highly compatible across the temperature range of application for PbTe based material. These materials are also very compatible with Bi_2Te_3 for functionally grading at lower temperatures and are indeed better than previously thought for PbTe and Bi_2Te_3.[21,57] Using optimally doped $PbTe_{1-x}I_x$ will result in increased thermoelectric efficiency of segmented elements and couples.

4 Summary

In summary, n-type PbTe samples doped with iodine were prepared and the measured electronic transport properties were shown to be agreeable with historically reported data for this material system. The common practice flash thermal diffusivity technique was used for measurements to 800 K and results in significantly lower thermal conductivity values than older measurement methods. The combination of precise control of the doping level and reliable thermal conductivity measurements reveals a large figure of merit of 1.4 between 700–850 K, which is substantially larger than commonly referenced for this historical material. Such a high zT within this temperature range is inherent to PbTe and likely contributes to high zT values measured using the same techniques on similar material systems.[5,28,58–62]

Acknowledgements

This work is supported by NASA-JPL and DARPA Nano Materials Program.

References

1 A. Ioffe, *Semiconductor Thermoelements and Thermoelectric Cooling*, Infosearch, London, 1957.
2 R. Abelson, *Thermoelectrics Handbook: Macro to Nano*, CRC/Taylor & Francis, Boca Raton, FL, USA, 2006, ch. 56, pp. 1–26.
3 K. Hsu, S. Loo, F. Guo, W. Chen, J. Dyck, C. Uher, T. Hogan, E. Polychroniadis and M. Kanatzidis, *Science*, 2004, **303**, 818–821.
4 C. J. Vineis, A. Shakouri, A. Majumdar and M. G. Kanatzidis, *Adv. Mater.*, 2010, **22**, 3970–3980.
5 M. G. Kanatzidis, *Chem. Mater.*, 2010, **22**, 648–659.
6 Y. Pei, J. Lensch-Falk, E. Toberer, D. Medlin and G. Snyder, *Adv. Funct. Mater.*, 2011, **21**, 241–249.
7 Y. Pei, A. May and G. Snyder, *Adv. Energy Mater.*, 2011, **1**, 291–296.
8 Y. Ravich, B. Efimova and I. Smirnov, *Semiconducting lead chalcogenides*, Plenum Press, 1970.

9 J. An, A. Subedi and D. Singh, *Solid State Commun.*, 2008, **148**, 417–419.
10 E. Bozin, C. Malliakas, P. Souvatzis, T. Proffen, N. Spaldin, M. Kanatzidis and S. Billinge, *Science*, 2010, **330**, 1660–1663.
11 Y. Pei, A. LaLonde, S. Iwanaga and G. J. Snyder, *Energy Environ. Sci.*, 2011, DOI: 10.1039/c0ee00456a.
12 A. Petrov, *Thermoelectric properties of Semiconductors*, Consultants Bureau, New York, 1964, p. 17.
13 W. Parker, R. Jenkins, G. Abbott and C. Butler, *J. Appl. Phys.*, 1961, **32**, 1679.
14 R. Fritts, *Thermoelectric Materials and Devices*, Reinhold Pub. Corp., New York, 1960, pp. 143–162.
15 D. Snowden, *Insulator and materials for close-spaced thermoelectric modules*, Hi-z technology, inc. for US department of energy technical report, 2003.
16 R. Heikes, R. Miller and R. Ure, *Thermoelectricity: Science and Engineering*, Interscience Publishers, New York, 1961, pp. 405–442.
17 S. Freedman, *Direct Energy Conversion*, McGraw-Hill, USA, 1966, ch. 3, pp. 105–180.
18 F. Rosi, *Solid-State Electron.*, 1968, **11**, 833–868.
19 C. Wood, *Rep. Prog. Phys.*, 1988, **51**, 459–539.
20 V. Fano, *CRC Handbook of Thermoelectrics*, CRC Press, New York, 1995, ch. 21, pp. 261–266.
21 G. Snyder, *Thermoelectrics Handbook: Macro to Nano*, CRC/Taylor & Francis, Boca Raton, FL, USA, 2006, ch. 9, pp. 1–26.
22 D. Rowe, *Thermoelectrics Handbook: Macro to Nano*, CRC/Taylor & Francis, Boca Raton, FL, USA, 2006, ch. 1, pp. 1–14.
23 G. Snyder and E. Toberer, *Nat. Mater.*, 2008, **7**, 105–114.
24 I. Kudman, *Metall. Trans.*, 1971, **2**, 163–168.
25 Y. Gelbstein, Z. Dashevsky and M. Dariel, *Proc. 21st Int. Conf. Thermoelectrics*, 2002, 9–12.
26 Y. Gelbstein, Z. Dashevsky and M. Dariel, *Phys. B*, 2005, **363**, 196–205.
27 B. Abeles, G. Cody and D. Beers, *J. Appl. Phys.*, 1960, **31**, 1585–1592.
28 J. Androulakis, C. H. Lin, H. J. Kong, C. Uher, C. I. Wu, T. Hogan, B. A. Cook, T. Caillat, K. M. Paraskevopoulos and M. G. Kanatzidis, *J. Am. Chem. Soc.*, 2007, **129**, 9780–9788.
29 K. Ahn, M.-K. Han, J. He, J. Androulakis, S. Ballikaya, C. Uher, V. P. Dravid and M. G. Kanatzidis, *J. Am. Chem. Soc.*, 2010, **132**, 5227–5235.
30 A. LaLonde, T. Ikeda and G. Snyder, *Rev. Sci. Instrum.*, 2011, **82**, 025104.
31 R. Blachnik and R. Igel, *Z. Naturforsch. B*, 1974, **29**, 625.
32 J. P. Heremans, C. M. Thrush and D. T. Morelli, *J. Appl. Phys.*, 2005, **98**, 063703.
33 E. S. Toberer, A. F. May and G. J. Snyder, *Chem. Mater.*, 2010, **22**, 624–634.
34 S. Airapetyants, M. Vinograd, I. Dubrovskaya, L. Kolomoets and I. Rudnik, *Sov. Phys.-Sol. State*, 1966, **8**, 1069.
35 I. Chernik, V. Kaidanov, M. Vinogradova and N. Kolomoets, *Sov. Phys. Semicond.*, 1968, **2**, 645.
36 M. Zhitinskaya, V. Kaidanov and I. Chernik, *Sov. Phys.-Sol. State*, 1966, **8**, 246.
37 M. Vinogradova, I. Rudnik, L. Sysoeva and N. Kolomoets, *Sov. Phys. Semicond.*, 1969, **2**, 892.
38 Y. Ravich, B. Efimova and V. Tamarchenko, *Phys. Status Solidi B*, 1971, **43**, 11–33.
39 I. Smirnov and Y. Ravich, *Sov. Phys.-Sol. State*, 1967, **1**, 739–741.
40 H. Lyden, *Phys. Rev.*, 1964, **135**, A514.
41 Y. Ravich, in *Lead Chalcogenides: Physics and Applications*, ed. D. Khokhlov, Taylor & Francis Group, New York, 2003, pp. 1–34.
42 V. Kaidanov, R. Melnik, I. Chernik and A. Kosulina, *Sov. Phys. Semicond.*, 1969, **2**, 1474.
43 R. Tauber, A. Machonis and I. Cadoff, *J. Appl. Phys.*, 1966, **37**, 4855.
44 J. Bardeen and W. Shockley, *Phys. Rev.*, 1950, **80**, 72.
45 C. Herring and E. Vogt, *Phys. Rev.*, 1956, **101**, 944–961.
46 F. Herman, R. Kortum, I. Ortenburger and J. Van Dyke, *J. Phys. Colloq.*, 1968, **29**, C4-62–C4-77.
47 H. Sitter, K. Lischka and H. Heinrich, *Phys. Rev. B: Solid State*, 1977, **16**, 680.
48 Y. Pei, X. Shi, A. LaLonde, H. Wang, L. Chen and G. J. Snyder, *Nature*, 2011, **473**, 66–69.
49 C. Bhandari and D. Rowe, *CRC Handbook of Thermoelectrics*, CRC Press, Boca Raton, FL, USA, 1995, ch. 5, pp. 43–53.
50 T. Stavitskaya, I. Prokofev, Y. Ravich and B. Efimova, *Sov. Phys. Semicond.*, 1968, 952–956.
51 A. Veis, R. Kuteinikov, S. Kumzerov and Y. Ukhanov, *Sov. Phys. Semicond.*, 1976, **10**, 1320–1321.
52 T. Stavitskaya, V. Long and B. Efimova, *Sov. Phys.-Sol. State*, 1966, **7**, 2062–2063.
53 B. Efimova, L. Kolomoets, Y. Ravich and T. Stavitskaya, *Sov. Phys. Semicond.*, 1971, **4**, 1653–1658.
54 G. Alekseeva, E. Gurieva, P. Konstantinov, L. Prokof'eva and M. Fedorov, *Semiconductors*, 1996, **30**, 1125–1127.
55 I. Dubrovskaya and Y. Ravich, *Sov. Phys.-Sol. State*, 1966, **8**, 1160.
56 Y. Gelbstein, Z. Dashevsky and M. Dariel, *Proc. 20th Int. Conf. Thermoelectrics*, 2001, 143–149.
57 G. Snyder, *Appl. Phys. Lett.*, 2004, **84**, 2436–2438.
58 J. R. Sootsman, H. Kong, C. Uher, J. J. D'Angelo, C. I. Wu, T. P. Hogan, T. Caillat and M. G. Kanatzidis, *Angew. Chem., Int. Ed.*, 2008, **47**, 8618–8622.
59 J. R. Sootsman, J. He, V. P. Dravid, S. Ballikaya, D. Vermeulen, C. Uher and M. G. Kanatzidis, *Chem. Mater.*, 2010, **22**, 869–875.
60 J. R. Sootsman, D. Y. Chung and M. G. Kanatzidis, *Angew. Chem., Int. Ed.*, 2009, **48**, 8616–8639.
61 J. R. Sootsman, J. He, V. P. Dravid, C.-P. Li, C. Uher and M. G. Kanatzidis, *J. Appl. Phys.*, 2009, **105**, 083718.
62 C. Long, X. Hou, Y. Gelbstein, J. Zhang, B. Ren and Z. Wang, *Int. Conf. Thermoelectr., 25th*, 2006, 382–385.

